



## Research paper

# Turbine scale and siting considerations in wind plant layout optimization and implications for capacity density

Andrew P.J. Stanley<sup>\*</sup>, Owen Roberts, Anthony Lopez, Travis Williams, Aaron Barker

National Renewable Energy Laboratory, 15013 Denver W Pkwy, Golden, CO 80401, USA

## ARTICLE INFO

## Article history:

Received 27 September 2021

Received in revised form 8 January 2022

Accepted 20 February 2022

Available online xxx

## Keywords:

Wind plant layout optimization

Siting considerations

Setback constraints

Capacity density

Turbine scale

## ABSTRACT

Improvements in wind energy technology, reduced costs, and ambitious clean energy goals have led to projections of high wind contribution in coming years. Developing methodologies to design wind plants with a variety of siting constraints and turbine sizes helps enable high wind penetration, and gain a better understanding of how wind plants are sensitive to setback constraints and turbine design. In this paper, we present a two-step optimization method to simultaneously determine the optimal number of turbines and their locations in a wind plant domain divided into many small, discrete parcels. We present the optimized performance metrics of a wind plant optimized with different turbine sizes and ratings, and with different siting restrictions within the wind plant. Our results indicate that taller and larger turbines are more sensitive to increasing siting constraints. We also compare the optimal wind plant layouts and performance for wind plants optimized for minimum COE and maximum profit. Wind plants optimized for profit had 130%–190% of the capacity of plants optimized for COE, which demonstrates that the optimal results are greatly affected by the objective function, which should be carefully considered. Finally, in this paper we demonstrate the effect of increasing siting constraints on wind plant capacity density, and how the results change when different land areas are used to calculate capacity density. When using the entire wind plant boundary area to determine capacity density, increasing siting constraints decreases the capacity density. However, when we only use the available area (the area left after removing the siting constraints) to calculate the capacity density, increasing the siting constraints increases capacity density. This is a critical insight because of how capacity density is typically defined and used in research, and has important implications for assessment of technical potential and capacity expansion modeling, as well as future wind deployment potential.

© 2022 The Author(s). Published by Elsevier Ltd. This is an open access article under the CC BY license (<http://creativecommons.org/licenses/by/4.0/>).

## 1. Introduction

Clean energy ambitions and declining costs are helping to drive current wind deployment in the United States, potentially leading wind energy to be a major contributor to the U.S. electric power system over the next several decades. The potential for wind energy to be a major contributor to U.S. electric needs has been demonstrated through sophisticated capacity expansion models (Cole et al., 2020; Center, 2020; Williams et al., 2021) that optimize regional wind resources with local energy demand, cost, and competition among other energy-generating technologies. Underpinning these capacity expansion models are geospatial assessments of wind technical potential, which capture the quantity, quality, and cost of evacuating the site-dependent resources to the electric grid. Previous estimates of wind technical potential have collectively concluded that the United States does indeed have enough wind resource to meet even the most

stringent clean energy targets (Lopez et al., 2012, 2021; Eureka et al., 2017). However, recent wind technical potential literature, through use of unprecedented spatial resolution, has illuminated the effects that local siting challenges could have on significantly lowering wind potential (Lopez et al., 2021). Further, a companion journal article to Lopez et al. (2021) demonstrated how these local siting constraints could result in a diminished wind energy contribution, increased energy costs, and slower CO<sub>2</sub> emissions reductions (Mai et al., 2021). These manuscripts highlight the need for more detailed spatial modeling to capture siting constraints faced by wind developers and their effects on national deployment projections. They also take a step forward in evaluating how wind turbine innovation may play a key role in unlocking wind potential when faced with limited siting options.

While those recent manuscripts highlight the importance of the challenges and advance methods for capturing detailed spatial constraints, they do not fully capture interactions between turbine innovation and varying siting conditions, which the authors noted as a limitation and also called for in Nitsch et al. (2019). This limitation is apparent in the literature, as there is a reliance

<sup>\*</sup> Corresponding author.

E-mail address: [pj.stanley@nrel.gov](mailto:pj.stanley@nrel.gov) (A.P.J. Stanley).

on estimating wind capacity through use of a constant capacity density estimate. Capacity density is a simple relationship between available land area and the amount of capacity that could be deployed, represented as MW/km<sup>2</sup>. Capacity density is generally determined through empirical assessment (Denholm et al., 2009) or through rotor-based spacing requirements (Rinne et al., 2018). Although these methods have been used throughout the literature to determine wind technical potential, they have significant limitations. Specifically, empirical estimates are based on a historic fleet of wind turbines and do not enable the exploration of wind turbine innovations (e.g., taller towers). Further, studies often rely upon a national mean capacity density even though regional variations exist in the empirical data (Lopez et al., 2021). Second, other literature derives capacity density from rotor-based spacing requirements (Rinne et al., 2018), which generally assumes a uniform grid of turbines and does not enable the assessment of wind energy as it is deployed in relation to landscape features, land use and ownership patterns, and the built environment. These methods have historically enabled us to explore wind energy's potential. However, there is a need for more sophisticated methods to enable us to capture location-specific deployment opportunities while simultaneously modeling the interaction of specific turbine designs. This is particularly important in siting constrained environments and under a deep decarbonization future, in which there is a tension between limited land availability and massive required deployment.

The need for this research is driven by innovation, which frequently results in increased wind turbine size and scale as well as projections of high wind deployment in the future potentially in locations with higher structure densities. More specifically, turbine tip heights and ratings are increasing which, as we show, will potentially decrease deployed capacity potential for land constrained sites and will increase the complexity of siting turbines for all sites with structures or infrastructure. We find that wind plant design and performance is sensitive to each of the drivers we study including: turbine scale, setback requirements, and objective function.

In this paper, we present three major contributions. First, we introduce a novel two-step optimization methodology to optimize wind plant layouts with varying degrees of siting restrictiveness. For a variety of reasons, wind plants are required to have some minimum spacing between turbines and different infrastructure and geographic features within the boundary of the plant. These minimum spacing requirements are called setbacks. In a wind plant, requiring certain setbacks to different structures within the plant boundary often results in a domain that is divided into several discrete parcels. Performing layout optimization in this domain is extremely difficult. Second, we present our results on how optimal wind plant design and performance is sensitive to different factors, and what the implications are for capacity density assumptions. We consider turbine scale, or how the physical height and rotor diameter of a turbine, affect how they are placed. We consider different setback requirements, and how different turbine sizes are sensitive to decreases in available area in which to site turbines. We also consider two objective functions, cost of energy (COE) and profit. COE is a standard objective in research, where for wind farm developers financial profitability is a more representative objective. Third, we explore the sensitivity of capacity density based on the assumed available development area, which can drastically influence downstream technical potential estimation and capacity expansion modeling. Some of the main takeaways of this research are: taller turbines require larger absolute physical distances from structures and infrastructure, and are therefore more sensitive to decreases in available area from increasing setback requirements defined with a tip height multiplier; because increasing setback requirements

reduces the available area in which to build turbines, it can reduce the capacity of a wind farm depending on the objective and the limitations on land availability; and wind plants optimized for maximum profit have higher capacity than those optimized for minimum COE.

The findings in this paper are an important first step in understanding some of the interactions and sensitivities of turbine scale and setback constraints and their implications for capacity density. We have not yet considered further innovations that enable more flexible siting, such as wake steering which will allow turbines to be built closer together, flicker and noise mitigation with advanced plant controls which may reduce setback requirements, and co-located wind and solar plants that could benefit from some of the advantages of each generation source. Considering these innovations, and others, will affect the sensitivities and relationships that we explored in this research.

The rest of this paper is outlined as follows. In Section 2, we describe our study area, turbine assumptions, wake model and power calculations, and then our siting restrictions. In Section 3, we describe our optimization methods and objectives. In Section 4, we present model outcomes organized by optimal layouts, optimal metrics, and capacity density. Lastly, in Sections 6 and 7, we conclude the report and offer implications for future research regarding wind energy's potential.

## 2. Models

This section includes descriptions of the models used in this paper, including assumptions about the wind plant domain, wind turbine models, the wake model, and the wind resource.

### 2.1. Blue creek wind farm

For this study, we used land features from the Blue Creek Wind Farm, which is an operational plant in northwest Ohio in the United States. An aerial view of Blue Creek is shown in Fig. 1. In order to reduce the required computational expense for the optimizations, we selected a smaller section of roughly 62 km<sup>2</sup> within the plant boundary, as represented by the blue square in Fig. 1. Fig. 2 shows a representation of the important land features that we considered for this study. These features require minimum setback constraints in our layout optimization to imitate land-use regulations, and include railways, roads, transmission lines (HIFLD Open Data, 2020), and buildings (Microsoft, 2020).

To simplify our layout optimizations, we assumed that all land is available for wind plant development after the setback constraints are met. This means there are no additional land features, exclusions, or non-participating landowners that further limit the land area. However, it would be a simple step to include any additional limitations on the land availability.

### 2.2. Wind turbines

In this paper we show results for wind plant optimizations with three different wind turbines, with the intent to capture differences in optimal results as affected by the turbine size and cost. The three turbines approximately represent what the onshore turbines of the future could look like with different amounts of innovation: conservative, moderate, and advanced. The likelihood of each turbine design coming to fruition decreases as the required innovation increases. In this work, the small conservative turbine is modeled after existing 2018 turbine technology (Stehly and Beiter, 2020), whereas the moderate and advanced turbine designs are from the 2020 Annual Technology Baseline (ATB) assessment for potential turbine designs in 2030 (NREL, 2020) from the National Renewable Energy Laboratory (NREL).

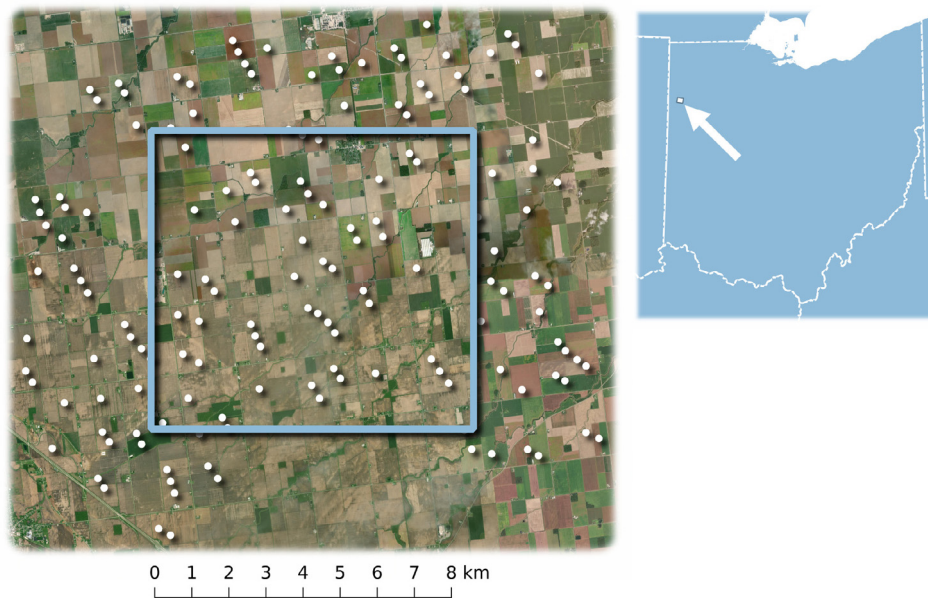


**Fig. 1.** A satellite image of the Blue Creek Wind Farm. The blue box represents the study area for this paper, and the white dots represent all existing turbines within the full extent of the plant. The small figure on the right shows the location of the Blue Creek Wind Farm to scale in Ohio, USA.

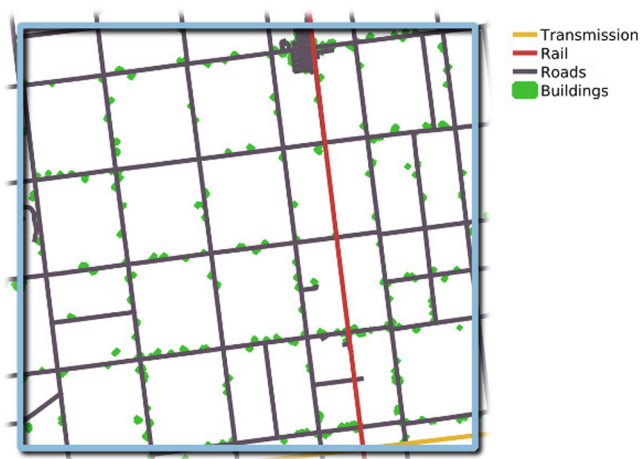


**Fig. 2.** A representation of the domain analyzed in this paper. Shown are the features that require setbacks during turbine layout optimization—buildings, roads, transmission lines, and railways. Features are exaggerated in size for visibility.

The turbine configurations for this work were selected for consistency with the ATB and previous work by Lopez and Mai on these same turbine configurations in estimating technical potential and under future capacity expansion scenarios. Lopez et al. 2021 found that moderate and advanced turbines could lose 14% and 20% capacity potential nationally, respectively, compared to existing (conservative) turbine technology, a result driven by larger setbacks (less area available) for larger rotors (Lopez et al., 2021). However, the amount of national generation remained within 1% among all turbines, even with substantially less capacity, due to increased capacity factors resulting from higher hub heights of the moderate and advanced turbines. These results indicate that higher hub heights may alleviate siting constraints, although this is confounded by the use of a single capacity density among all turbines as we demonstrate in this paper. Mai et al. 2021 found that for both the moderate and advanced turbines, increasing siting restrictiveness resulted in significant drops in

wind energy contribution to the future electric system (Mai et al., 2021).

Fig. 3 shows the important characteristics of each turbine used in this study. The top row visually represents each turbine and displays the rotor diameter and hub height. The second row shows the power curve for each turbine, from which we can see that the rated powers for the turbines are 2.43, 5.5, and 7 MW for the conservative, moderate, and advanced turbines, respectively. For each turbine, the cut-in wind speed is 3 m/s, rated wind speed is 10 m/s, and the cut-out wind speed is 25 m/s. The third row shows capital expense cost curves for each of the turbines, and demonstrates economies of scale associated with building larger wind plants. These curves were created using the detailed balance of station (BOS) cost model LandBOSSE, which is based on current construction practices and technology and results in larger economies of scale for larger turbines and higher capacity wind plants (Eberle et al., 2019). The ATB inputs within the BOS cost model also predict dramatic decreases in turbine costs with increasing turbine innovation, which we captured in this research.

### 2.3. Setbacks

We modeled the setback requirements in this paper as a multiple of the wind turbine tip height, which is common in many local regulations. The tip height is the maximum height of the turbine structure, which is the hub height plus the rotor radius. Additionally, we assumed that the setback constraint is the same for each feature (e.g., buildings and roads). For this paper, we examined setback constraints of 0, 1.1, 2, and 3 times the turbine tip height from each feature. The land available for wind plant development for each setback multiplier and each turbine tip height is shown in Fig. 4. In this figure, the land that is still available after applying the setback constraints is shown in blue. The first, second, and third rows represent the conservative, moderate, and advanced turbines from Fig. 3, respectively, while each column represents a different setback multiplier. In the top right corner of each subfigure, there is a value that indicates the percentage of the total area that is still available after the setbacks. Note how limited the land area becomes with larger

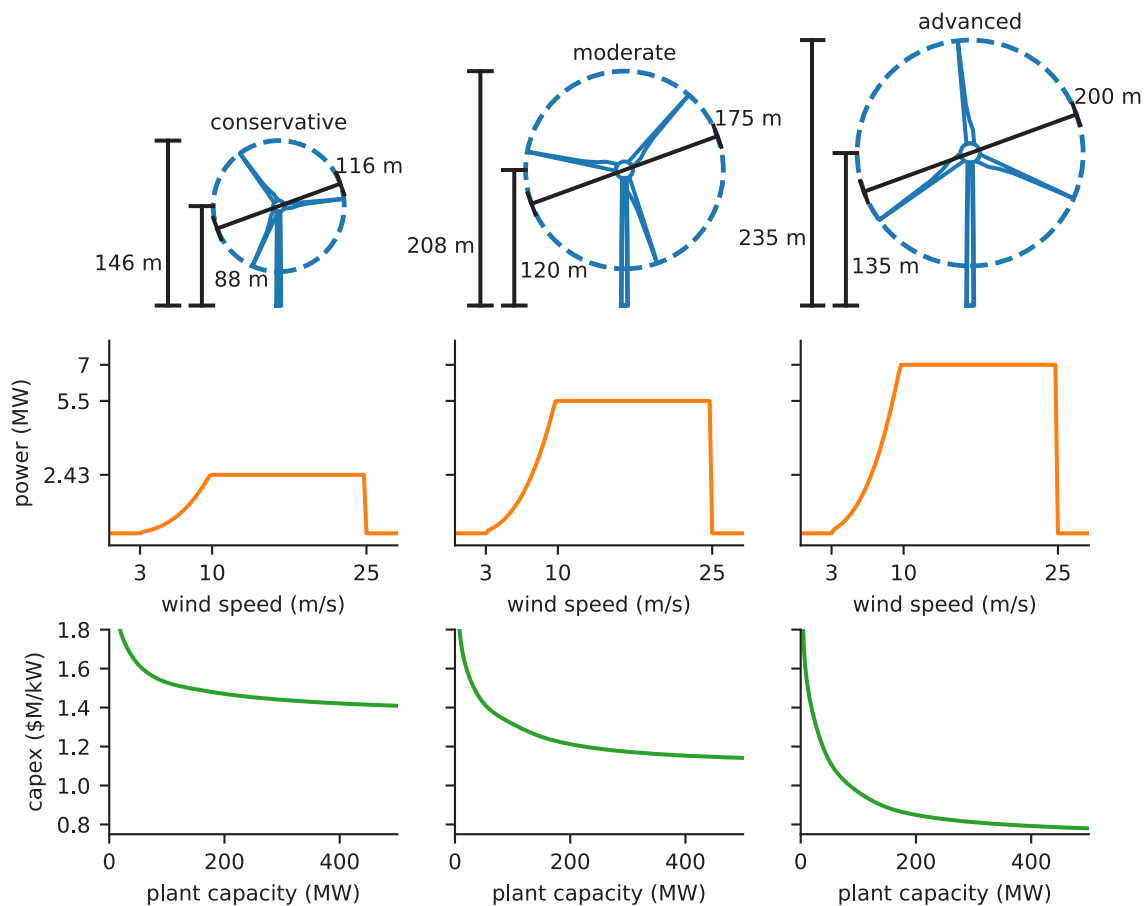


**Fig. 3.** The three different turbine models used in this paper. The first row shows the turbine sizes; the second row shows the power curves; and the bottom row shows the capital expense curves as a function of plant capacity. Each column represents turbine designs with conservative, moderate, and advanced innovation.

setbacks and larger turbines. For example, the land available for the advanced turbine with a setback multiplier of 3 is just 0.2%, or 1/500th, of the total wind plant area.

#### 2.4. Wake model and power calculations

To calculate the effective wind speeds at each turbine to use in the wind plant power calculations, we used the Jensen wake model (Jensen, 1983). Although the Jensen model is a simplified representation of the actual flow physics in the wind plant, it is sufficient for capturing the relative changes in wake losses and energy production for this effort for a low computational expense. This accuracy, along with the simplicity of the model and its widespread use in academia and industry, led us to select it. For actual design of a wind plant, we would recommend using a more accurate analytic wake model, or some higher fidelity method. However, for this paper the purpose is to demonstrate our methods and show high level trends. Thus, for this paper the Jensen wake model was sufficient. We would expect different wake models to have little effect on the optimal number of wind turbines. As is discussed in Section 3.3, the number of turbines is driven by the combination of a cost model and the wake model, not the wake model alone.

We performed the wind plant power calculations for this paper within NREL's HOPP platform, a freely available open-source tool for component-level design and optimization of utility-scale hybrid plants (Tripp et al., 2020). HOPP relies on another NREL software, the System Advisor Model (SAM) to perform the wind plant wake and power calculations (Freeman et al., 2018). The wind power performance model in SAM calculates the hourly

electrical output of a single wind turbine or of a wind plant. The wind power performance model requires information about the wind resource, wind turbine specifications, wind plant layout, and costs. This performance model can be coupled to one of the financial models to calculate economic metrics for residential, commercial, or utility-scale wind projects. We used HOPP as the means to run SAM in this wind plant analysis to enable greater flexibility in component layout optimization, and to leave open the possibility of performing hybrid plant design in future work.

#### 2.5. Wind resource

In addition to using the Blue Creek Wind Farm for setback feature data, we also used the associated wind resource. We used the 2013 hourly resource data from NREL's WIND Toolkit (Draxl et al., 2015) for our wind plant models. Fig. 5 shows the directional wind frequency data, as well as the mean wind speed for each direction binned into 10-degree sections. For wind plant layout optimization, it is common to use the directionally averaged wind speeds instead of the full wind speed distributions to reduce computational expense, and is what we did in this paper. Although this wind resource is predominantly from the southwest, there are non-negligible resources from all directions.

### 3. Optimization methods

Even in its most basic form, wind plant layout optimization is a difficult problem. In the literature, when performing wind plant layout optimization, previous studies show a preference for gradient-free optimization methods—different studies have



**Fig. 4.** The available area remaining in the wind plant domain with different setback requirements from various features. Each column represents different setback requirements of 1.1, 2, and 3 times the turbine tip height, and each row represents a different turbine design (corresponding to the turbines represented in Fig. 3). The shaded blue areas represent the areas where turbines can be built, and the percentage in the top right corner of each subfigure shows the percent of the total land area still available after applying the setbacks.

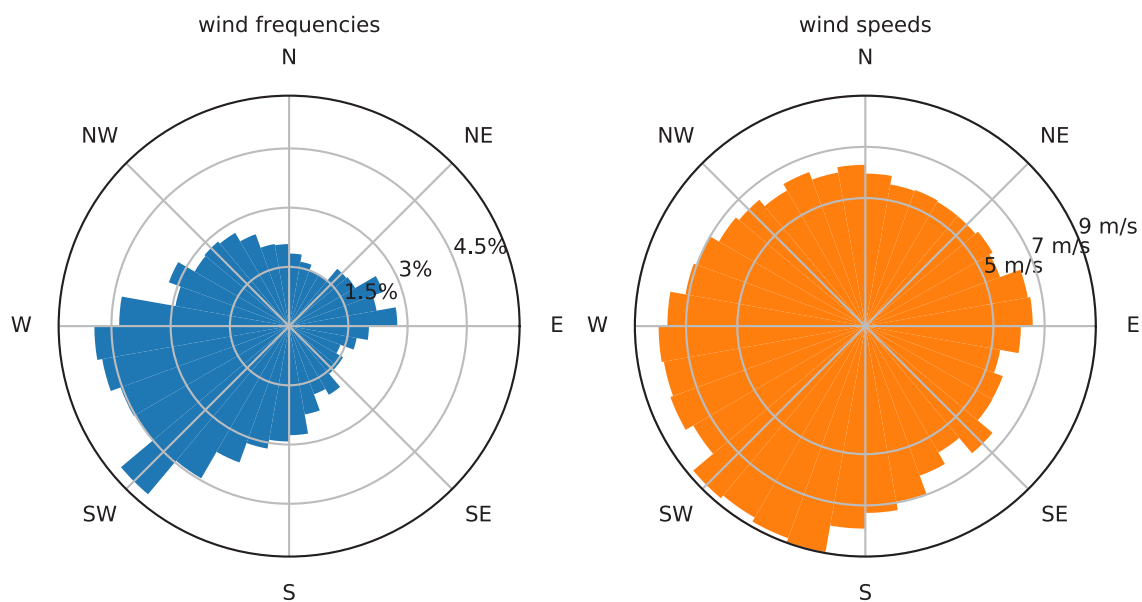


**Fig. 5.** The wind resource data from the Blue Creek Wind Farm. On the left are the wind frequency data, and the right shows the wind speeds averaged for each wind direction bin.

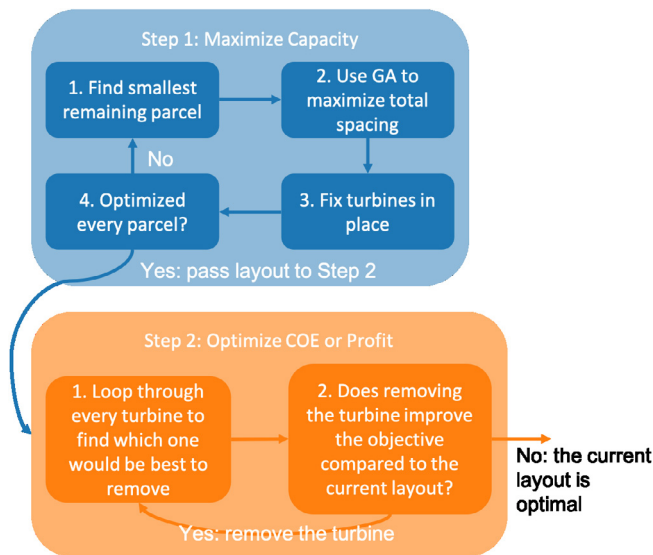


Fig. 6. A diagram visualizing our two-step optimization method.

demonstrated successful optimization using genetic algorithms, particle swarm methods, and random search to improve wind power plant layouts (Hou et al., 2019). Gradient-free optimization methods have also been demonstrated to have great success and computational efficiency when optimizing a wind plant (Thomas and Ning, 2018; Baker et al., 2019). Often in wind plant layout optimization studies, the number of turbines is assumed to be known before performing the layout optimization. Including the number of turbines within the optimization greatly increases the complexity of the problem and effectively forces the use of a gradient-free optimizer (Stanley et al., 2021). Further complexity is introduced when the wind plant domain is large, and has separate, discrete areas in which turbines can be built. Although it has not been explored in depth, there are a few studies in the current literature which include optimization of a wind plant layout where the boundary has been split into multiple sections. The wind plant layout optimization portion of IEA Task 37 (Baker et al., 2021) is currently looking into different methods that could be used to solve this optimization problem. Additionally, some studies on wind plant layout optimization with landowner participation have performed some preliminary exploration into possible strategies to solve this complex problem (Chen and MacDonald, 2011, 2012, 2013, 2014; Wang et al., 2017). Like the setbacks in our problem, varying degrees of landowner participation can also divide a wind plant into several discrete parcels. The current literature on this topic provides an excellent starting point to develop the necessary optimization methods required for this paper. The methods we present in this paper build on what has already been accomplished. We present an strategy to find optimized turbine layouts with a large number of divisions with sections that have large size variations.

In this paper, we optimized the layout of turbines as well as the number of turbines, which is a discrete variable. Additionally, as seen in Fig. 4, the setback constraints effectively split the wind plant into several discrete parcels, which further complicates the problem. In order to optimize the number and layout of turbines in this complex domain, we developed and applied novel optimization techniques and strategies, which we will describe and discuss in this section. Our presented optimization strategy is divided into two steps and is shown in Fig. 6. Each step is detailed in Sections 3.1 and 3.2.

### 3.1. Step 1: Maximize capacity

#### 3.1.1. Method

The first step in our layout optimization is to maximize the capacity, or the number of turbines, that can fit in wind plant without violating the turbine spacing constraints for a given turbine design. This step in itself has several substeps that were determined by a series of trials:

1. Starting in the smallest parcel, maximize the number of turbines in the parcel
2. Fix the turbines from the previous parcel in place, and maximize the number of turbines in the next smallest parcel
3. Repeat until all parcels have been optimized.

In order to create land parcels that do not violate the setback constraints and calculate the parcel areas, we used the Shapely Python package for manipulation and analysis of planar geometric objects (Gillies et al., 2007).

To optimize the turbines in each parcel, we used a simple gradient-free method similar to that first introduced by Mosetti (Mosetti et al., 1994). This method works by creating a grid of potential turbine locations within the wind plant domain. Each of these grid locations is assigned a binary value, indicating whether a turbine is placed at the associated location. A gradient-free algorithm is then used to determine the optimal number of turbines and their locations. To create our grid locations, we created a square grid that spanned the minimum and maximum Cartesian  $x$  and  $y$  coordinates of the parcel in question. Then, because the parcels were irregular in shape, any of these grid points that were outside the parcel were moved to the nearest point on the parcel boundary to ensure that no grid points violated boundary constraints. This resulted in a larger portion of points being grouped around the boundary, which was likely advantageous as optimal wind plant layouts often have turbines on or near the boundary (Stanley and Ning, 2019b). The potential grid used approximately one rotor diameter spacing. Fig. 7 shows the grid points of 256 potential turbine locations that were used in our optimization for one larger parcel with the smallest wind turbine. Smaller parcels and larger turbines result in significantly fewer points.

To optimize the placement of turbines, we used a simple genetic algorithm. We used single point crossover, with the chromosome bits arranged sequentially, such that adjacent bits corresponded to adjacent turbine location points. Additionally, we used a mutation rate of 0.01, and a population size of 100. After performing the crossover and creating the offspring, we combined the parent and offspring populations and ranked them from best performing to worst performing. We kept the 100 best performing individuals from this list and used them as the parents for the subsequent generation. Although this strategy of only keeping the best performing individuals can result in inadequate exploration of the design space in some problems, for this problem the convergence occurred in few enough generations that this was not an issue. We determined that the algorithm converged if 100 generations passed with the best solution improving by less than an absolute tolerance of  $10^{-6}$ . In order to lend further confidence that we approached the global solution with our optimization algorithm, we repeated the genetic algorithm 10 times for each parcel with each individual in the population randomly initialized with one wind turbine.

We found that optimizing the smallest parcel first and working up to the larger parcels was the superior approach, compared to the optimizing the largest parcels first, or randomizing the order in which the parcels were optimized. The smallest parcels had very little freedom in where to place turbines compared to the

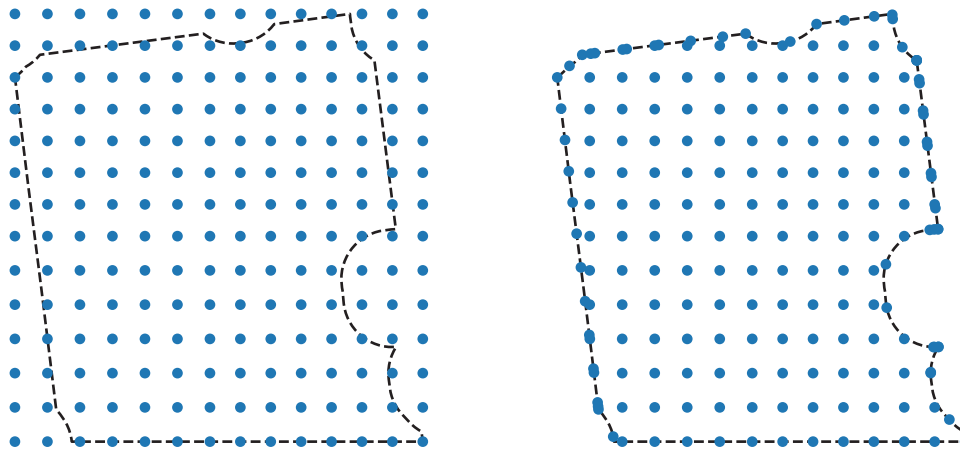


**Fig. 7.** An example of the grid of potential turbine locations for one land parcel. First, a regular square grid was placed that spanned the horizontal and vertical extremes of the land parcel. Then, any of these grid points that were outside of the boundary were moved to the closest point on the boundary to ensure that none of the points violated the boundary constraints. These points represent proposed locations where a turbine could be built, not actual turbine locations. We used a genetic algorithm to decide at which of these locations a turbine should be placed.

larger parcels (refer to Fig. 4, taking note of the difference in size of some of the smallest parcels and the largest ones). Thus, by optimizing the smaller parcels first, we prioritized placing at least one turbine in these areas if it could be achieved without violating spacing constraints with already placed turbines. After this, many turbines could still be placed in the larger parcels as there was more freedom to meet the spacing constraint. By optimizing the larger parcels first, turbines would often be placed close to the smaller parcels, so by the time the smaller parcel was optimized no turbines could be placed without violating spacing constraints.

### 3.1.2. Objective for step 1

For this capacity optimization, we used an objective of maximizing the total sum of spacing between all wind turbines. Maximizing the total spacing between turbines is superior to simply using a packing algorithm to maximize the number of turbines. The spacing maximization also acts as a basic energy production optimization because wake effects are generally reduced as spacing between turbines increases, but at greatly reduced computational expense. The spacing computation is much cheaper than a full evaluation of the wake model and power calculations, leading to huge computational savings over the entire optimization. We calculated the spacing objective with respect to all of the turbines in the wind plant, not just the turbines in the parcel being optimized. The optimizer could improve the objective by spreading the turbines farther apart and by adding more turbines. Therefore, the optimizer maximized the capacity of the wind plant while also accounting for some interactions between turbines. This spacing objective is shown in Eq. (1).

$$\text{spacing objective} = \sum_{i=1}^n \sum_{j=1}^N d_{i,j} \tag{1}$$

In this equation,  $n$  is the number of turbines in the parcel being optimized,  $N$  is the number of turbines in the entire wind plant, including those in the parcel being optimized, and  $d_{i,j}$  is the distance between a turbine inside the parcel being optimized and another turbine in the plant.

### 3.1.3. Constraints

The only explicit constraint that we included in this optimization was a minimum turbine spacing of five rotor diameters between turbines in the plant. By moving all of the potential turbine location points inside each parcel boundary as shown in Fig. 7, we guaranteed that the setback and outer wind plant

boundary constraints are automatically satisfied. Because of this, additional explicit considerations did not need to be made for these turbine siting constraints. In all, this optimization problem is expressed in Eq. (2).

$$\begin{aligned} &\text{maximize} && \text{spacing objective} \\ &\text{w.r.t.} && \text{turbine locations} \\ &\text{subject to} && \text{spacing constraints (explicit)} \\ &&& \text{setback constraints (implicit)} \\ &&& \text{boundary constraints (implicit)} \end{aligned} \tag{2}$$

### 3.2. Step 2: Optimize COE or profit

In Step 1, for the objective of wind plant capacity and most of the time for energy maximization objectives, the optimizer will place as many turbines into the wind plant as possible, without violating spacing constraints. For other objectives, where there is a penalty for losses from turbine wakes, fewer turbines may be optimal. To optimize for these other wind plant objectives that sought to space turbines further apart, we started with the turbine layouts achieved by maximizing the wind plant capacity. These starting wind plant layouts for each setback multiplier and tip height after maximizing the wind plant capacity are shown in Fig. 8. In this figure, the black dots represent the wind turbines to scale, with the diameter representing the rotor diameter. Similar to the mesh of points that were created to optimize the turbine locations in each parcel (shown in Fig. 7), the turbine locations from the capacity maximized wind plants were used as potential turbine locations for optimizing other objectives. We then used a gradient-free optimizer to determine the optimal locations to place wind turbines.

We tested the use of two gradient-free optimizers to place the turbines in this step. One was the simple genetic algorithm that we used in the capacity optimization, except with a population size of two times the potential turbine locations instead of a constant 100 as we used for the capacity optimization. All of the other parameters were the same. The other optimizer we used was a greedy turbine removal algorithm. For this removal algorithm, we started with a turbine placed at every potential turbine location. We then removed the single turbine that resulted in the largest objective improvement. We repeated this process until removing a turbine no longer resulted in an improvement in the objective. For every wind plant optimization with the COE objective, we tested both of optimizers. For every

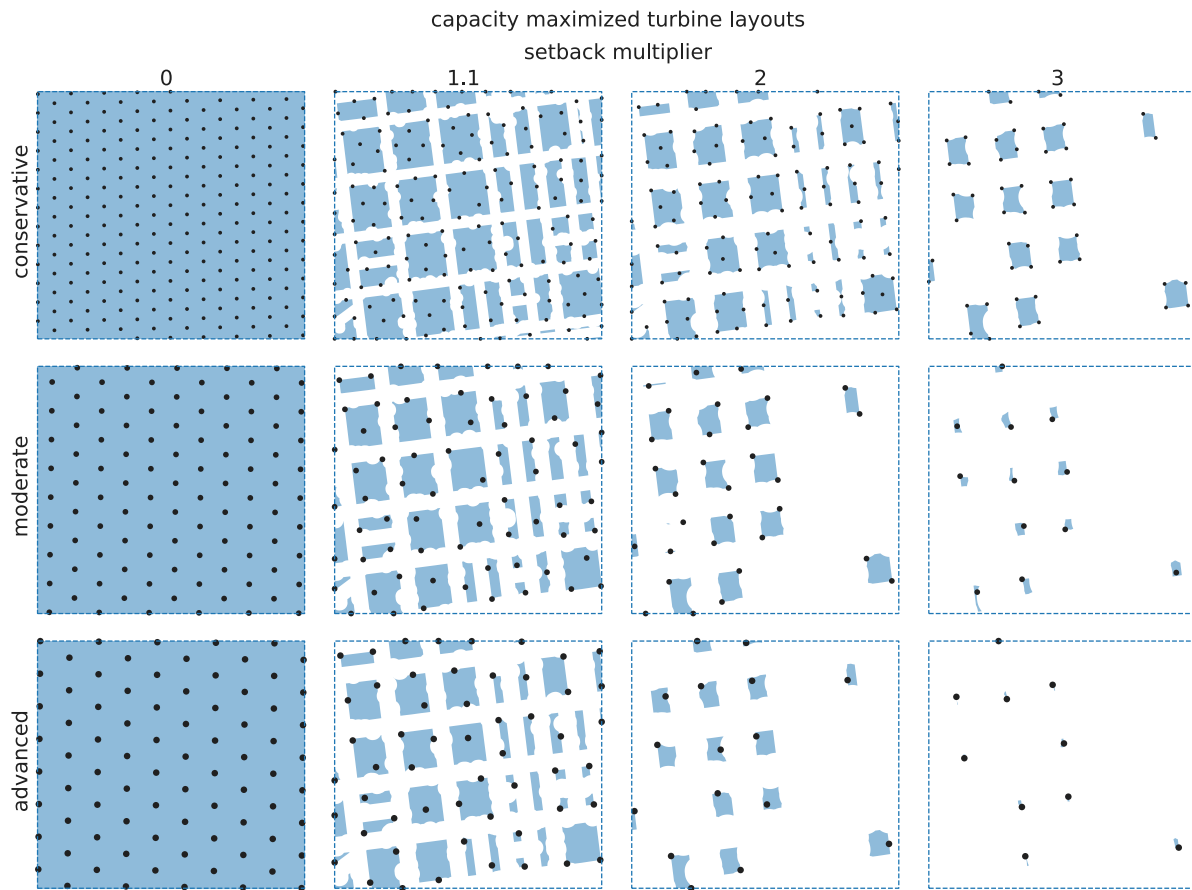


**Fig. 8.** Optimized wind plant layouts for a maximum capacity objective. The objective for this optimization was to maximize the sum of the spacing between all of the turbines, so these layouts are also a rough approximation of a maximum AEP layout. The turbines in these wind plants are spaced very close together and operate inefficiently. In this paper, these layouts are not final, but are used as an intermediate step before the final optimizations. The rows from top to bottom show the conservative, moderate, and advanced innovation turbines, where the size of each black dot is to scale representing the turbine rotor diameter. The columns from left to right show setback tip height multipliers of 0, 1.1, 2, and 3.

optimization, the final solution function values were within 0.03% of each other. Thus, because of the simplicity of the algorithm and good performance, we used the greedy removal algorithm for the results in this paper. We also briefly tested a greedy addition algorithm, which underperformed compared to the greedy removal algorithm. Although the addition algorithm was much faster than the removal one, the final solution depended on the starting condition, or the location of the first turbine to be placed, and generally performed significantly worse.

At this point in the optimization, additional improvement could be achieved by fine-tuning the location of the turbines with a gradient-based optimizer. We did not perform this fine-tuning for this paper, as we are more interested in the higher-level trends from the results of the optimization.

So, because the boundary and turbine spacing constraints were already applied in the capacity maximization step and turbines could only be placed in these locations, these constraints were automatically met in this phase of the optimization. No additional constraints were applied.

### 3.3. Objectives for step 2

Using the optimization method described in Section 3.2 we optimized two different objective functions: minimize COE defined in Eq. (3), and maximize annual profit defined in Eq. (4).

$$COE = \frac{\text{annual cost}}{AEP * (1 - L)} \tag{3}$$

$$\text{annual profit} = (AEP * (1 - L)) * PPA - \text{annual cost} \tag{4}$$

In these equations, AEP is the annual energy production, calculated in HOPP with the resource data shown in Fig. 5,  $L$  are any losses experienced within the plant, and PPA is the power purchase agreement. We assumed a constant value  $L = 8.8\%$ , and that the PPA is a constant although it can be varied between optimizations. For the purposes of this paper, the annual cost is defined in Eq. (5).

$$\text{annual cost} = FCR * CapEx + O\&M \tag{5}$$

In this equation, FCR is the fixed charge rate assumed to be 6.3%, CapEx is the wind plant capital cost (including turbine capital costs and balance of station costs), given by the curves in Fig. 3, and O&M are the operation and maintenance costs, which we assumed were \$37/kW of wind plant capacity. Eq. (5) is certainly a simplified expression to represent the plant costs. As with the other models presented in this paper, this cost model could be replaced with another with the desired complexity and fidelity. For our this paper, the presented expression is sufficiently realistic to demonstrate our methods and show high level trends and relationships.

For each of the objective functions, the model uses the relationships of wake losses and plant cost as a function of plant capacity and turbine layout to minimize COE or maximize profit. The wake loss relationships are based on the turbine layout and turbine type, captured by the Jensen wake model. The relationship of plant cost to capacity is derived for each turbine using the



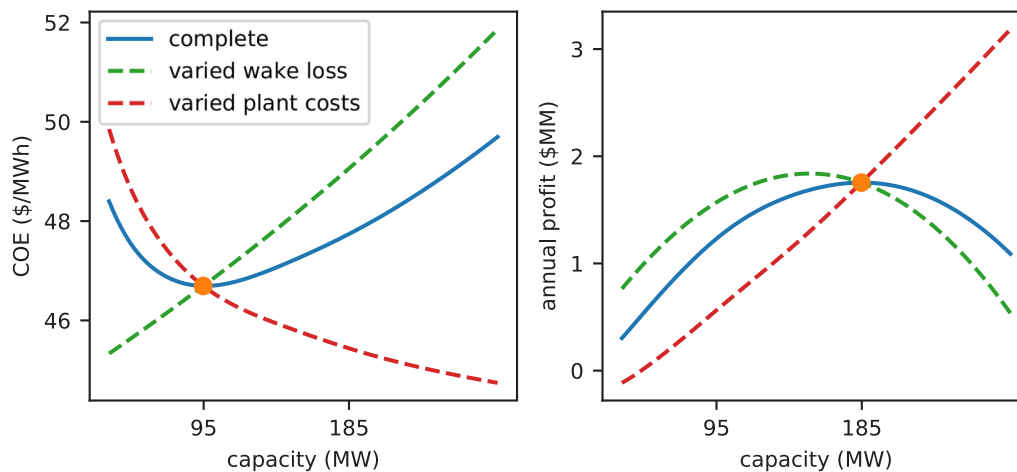


**Fig. 9.** The sensitivities of each objective function to wind plant capacity, and how the objectives balance competing interests. Each objective shows how the value changes if just the wake losses are varied with increasing capacity with no economies of scale, and how the value changes if just the unit costs are varied and the wake losses remain constant with increasing capacity. They also show the complete objective with increasing capacity.

NREL land-based wind BOS model LandBOSSE (Eberle et al., 2019). These cost curves are shown in Fig. 3. The objectives of COE and profit both try to maximize production and minimize the costs of the wind plant. However, the way each objective handles the competing interests is different. Both try to balance the trade-offs from increasing wake losses and decreasing unit costs as plant capacity increases. Fig. 9 illustrates the change in COE and profit due to plant cost scaling and wake losses as a function of capacity for the conservative innovation turbine. To make this figure, we created a wake loss relationship with quadratic curve fit to wake losses from 24 optimized wind plant layouts. With the wake loss curve, we calculated AEP as a function of wind plant capacity by assuming a constant capacity factor of 0.375, shown in Eq. (6).

$$\text{AEP} = 8,760 * \text{CF} * c * (1 - l_w) \quad (6)$$

In this equation, 8,760 is the number of hours in a year, CF is the capacity factor,  $c$  is the wind plant capacity, and  $l_w$  is the wake loss. This AEP calculation, along with the cost curve shown in Fig. 3, allowed us to create one-dimensional relationships of COE and profit as a function of capacity, from Eqs. (3) and (4). In addition to showing the one-dimensional COE and profit curves as a function of plant capacity, Fig. 9 also shows how each of these objectives is driven by the increasing wake losses associated with larger capacity, and the decreasing unit costs associated with capacity. The dashed lines show the values of each objective while either holding the unit plant costs constant and only varying wake losses with capacity, or holding the wake loss constant and only varying the unit plant costs with capacity.

Fig. 9 shows how plant capacity affects wake losses and cost economies of scale, and ultimately the objectives of COE and profit. In general as the plant capacity decreases, the relative plant costs increase due to economies of scale of plant construction (resulting from mobilization costs, electrical collection, interconnection costs, and other nonlinear relationships). Inversely, these relationships cause lower unit costs as plant capacity increases (Eberle et al., 2019). This economy of scale relationship incentivizes the optimizer to add as many turbines as possible to the area, and improves both objectives by adding more turbines. This relationship is shown by the red dashed lines in Fig. 9. On the other hand, wake losses increase with increased capacity as the average distance between turbines decreases. Increasing wake losses result in lower energy capture, and therefore higher COE and decreasing profit. The relationship that results from holding the costs constant but varying wake losses with capacity is shown by the green lines in the figure. The optimal solution

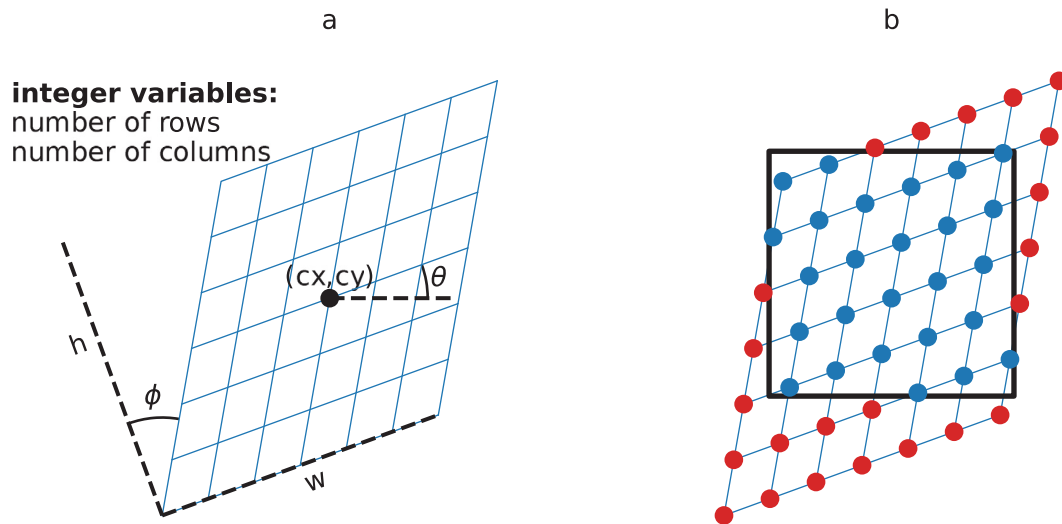
for each objective occurs where the improvement in AEP and cost reduction from adding additional capacity is outweighed by the decrease in efficiency from additional wake losses.

Fig. 9 is meant only to give a simple representation of how each objective behaves relative to capacity. In reality the problem is more complex, as the siting of turbines and setback constraints largely drive the wake losses in a plant. These relationships and sensitivities are discussed throughout the rest of the paper.

Our study assumes a scenario where the boundary area is fixed—typically referred to as a “land constrained” site. This fixed boundary area enables the wake loss and plant cost function to allow the optimization to find a solution. Many wind plants are constrained by the available capacity of the transmission line that the plant will connect to but without a constraint of available area. This scenario is typically referred to as a “capacity constrained” scenario. We do not include a cost relationship for varying the distance between turbines to account for increased road, collection system, crane travel time, or land lease cost, but including this cost relationship would allow for the optimization of capacity constrained sites.

### 3.4. Zero setback optimization

To provide points of comparison, we also performed turbine layout optimization with zero setbacks, meaning that the turbine layouts were only restricted by the boundary and spacing constraints. We again performed a two-step optimization process as was previously described, with the simplification of using a grid turbine layout parameterization for the capacity maximization step. Without any setback constraints, there is only one discrete parcel where turbines can be placed. This would require thousands of potential turbine location dots (as shown in Fig. 7) to sufficiently resolve the domain, which is too many to be efficiently optimized with the genetic algorithm used. Instead, we defined the wind plant layout in the zero setback case with eight grid variables: the number of rows and columns, the grid width and height, the grid offset or shear angle, the grid rotation, and the grid center  $x$  and  $y$  coordinate. These design variables are shown in Fig. 10a. Any turbines that fell outside of the wind plant boundary were removed, so the boundary constraint was met implicitly, as shown in Fig. 10b. After performing capacity maximization with the grid design variables, we used the previously discussed greedy turbine removal algorithm to optimize for the other objectives, as described in Section 3.2.



**Fig. 10.** A representation of the design variables used in the grid turbine layout optimization. Fig. 10a shows the 8 design variables used to define the grid, which are the grid height and width,  $h$  and  $w$ , the grid center coordinate,  $(cx, cy)$ , the grid shear,  $\phi$ , the rotation,  $\theta$ , and the number of rows and columns. Fig. 10b shows the turbines placed at the grid vertices, where the plant boundary is shown with the black square. The blue turbines are within the plant boundary, while the red turbines are outside of the boundary and are removed. (For interpretation of the references to color in this figure legend, the reader is referred to the web version of this article.)

## 4. Results and discussion

In this section, we present the results from applying our novel optimization method. We optimized wind plants for the objectives of minimizing COE, and maximizing profit. For each objective, we optimized the wind plant layout for the full combination of setback multipliers of 0, 1.1, 2, and 3, and conservative, moderate, and advanced innovation turbines, which totals 24 optimized wind plants. By performing this spread of optimizations, we were able to make conclusions about the sensitivities of the optimal solutions to different setback requirements for each different turbine design. In Section 4.1, we present the optimized wind plant layouts for each turbine, setback multiplier, and objective function, and in Section 4.2 we present and discuss the optimal metrics from each of the optimized wind plants. In this section we also explore the effect that the setback tip height multiplier has on optimized wind plant performance, and how this varies with turbine design.

### 4.1. Optimal wind plant layouts

In this section, we present and discuss the optimal wind plant layouts achieved for the COE and profit objectives. Fig. 11 shows the optimized wind plant layouts for a COE objective for each turbine design and setback constraint multiplier. By referring back to Fig. 8, we see that in general for this objective there are much fewer turbines than in the optimal wind plants for the capacity maximization objective. This is especially true for the wind plants with relatively large areas that are not as limited by setback constraints (lower setbacks and smaller turbines). The COE objective seeks to minimize the cost of wind plant development and operation while maximizing the energy production. The optimal number of turbines in the minimum COE solution occurs when the cost benefit from adding more wind turbines is outweighed by the extra wake losses that occur from adding more turbines to the plant.

Fig. 12 shows the optimized wind plant layouts for an objective of maximizing annual profit. In this figure, the black points represent the optimal COE turbine locations. These turbines are also present in the maximized profit layouts. The red points represent the additional turbines that exist in the maximum profit

layouts. As in Fig. 11, this figure shows the optimal layouts for each turbine and setback constraint. Because wind plant capital costs decrease significantly with increasing turbine innovation, we used a different PPA for each turbine such that the results were meaningful. We chose the PPA for each turbine design to be about 10% higher than the minimum COE solution for the zero setback case. We set these values early in our process, before each scenario had been fully explored, so the actual PPA values vary slightly from this target. These PPA values were 51.22, 38.91, and 30.27 \$/MWh for the conservative, moderate, and advanced innovation turbines, respectively. For the optimal profit layouts, in general there are more turbines than for the COE objective, but still fewer than for the capacity objective. For the profit objective, higher wake losses are more tolerable than in the COE objective. Even if the energy costs slightly more to produce per MWh, if additional turbines can add significant amounts of energy, it can result in a larger profit.

In both Figs. 11 and 12, we see that for the small setbacks of 0 and 1.1, the number of turbines is determined by the objective function. In other words, there are a lot of additional turbines in the layouts optimized for maximum profit for the small setback cases. There is enough freedom in placing the turbines that the optimal number of turbines is determined by the interaction between decreasing unit costs and increased wake losses from adding more turbines. However, as setbacks increase, the available land is reduced. In these situations the available parcels of land are very small, without much freedom to optimize their location and only allowing one or two turbines per parcel. Additionally, the number of discrete parcels is small, allowing fewer turbines to be placed than is optimal from a cost curve perspective. The number and location of the turbines in these plants is determined almost exclusively by the limited available land allowed from the setback constraints. In these cases, the optimal turbine locations for the COE and profit objectives are the same as for the capacity optimized plants. There are very few extra turbines in the layouts optimized for maximum profit, and in some case no extra turbines exist, simply because there is not enough space.

### 4.2. Optimal wind plant performance

In this section we discuss different metrics of each optimized wind plant, and the sensitivities of these metrics to the setback

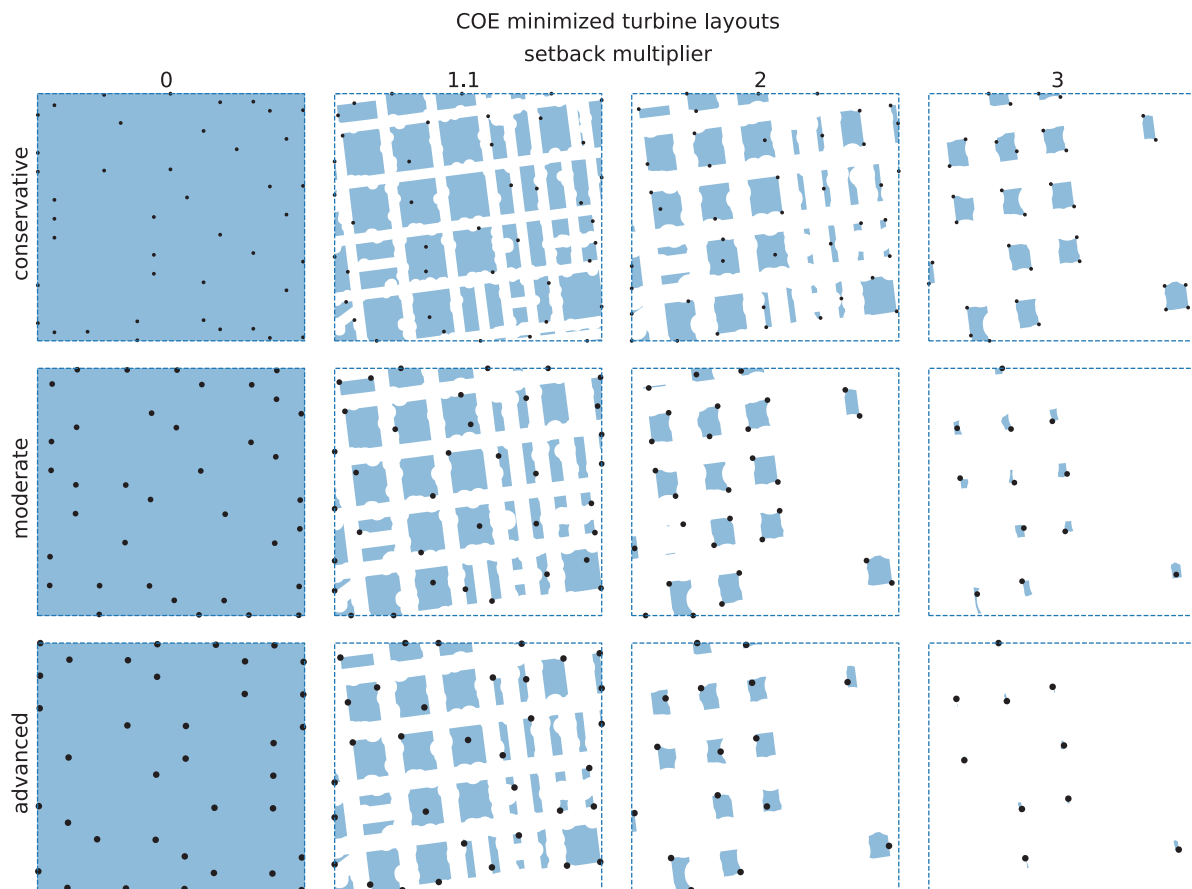


**Fig. 11.** The optimal wind plant layouts with the objective of minimizing COE. The rows from top to bottom show the conservative, moderate, and advanced innovation turbines, where the size of each black dot is to scale representing the turbine rotor diameter. The columns from left to right show setback tip height multipliers of 0, 1.1, 2, and 3.

constraint. Fig. 13 shows the results for the wind plant optimizations that minimized COE as their objective. For each optimized layout, this figure shows the number of turbines, total installed capacity (the product of the number of turbines and turbine rated capacity), AEP (the total energy production of all turbines minus any wake losses), COE, annual profit, and wake loss percentage. Results for the conservative, moderate, and advanced turbines are shown in the top, middle, and bottom figures, respectively.

An immediate observation from these results is that for the conservative and moderate turbines, the optimal COE with zero setback constraints is slightly higher than those with a setback multiplier of 1.1. This is simply an artifact of our turbine location definitions. Performing a gradient-based optimization to tune the locations of the turbines would result in a lower COE for the zero setback plants, or at least the same as that for the 1.1 setback plants. There is an enormous amount of additional information contained in Fig. 13, and many of the trends illustrated in this figure may be important for various applications. We will only explicitly point out and discuss the trends that we believe are most important. These trends are shown in Fig. 14, which shows the sensitivity of optimal wind plant capacity, COE, and wake loss as a function of the setback constraint.

First, we examine the relationship of optimal capacity with increasing setbacks constraints. When minimizing COE, there is no difference between the optimal capacity between the 0 and 1.1 setback cases for the conservative and moderate innovation turbines, and just a very small decrease in optimal capacity of about 5% for the advanced innovation turbine. This indicates that the optimal number of turbines to minimize COE can still fit within the wind plants with a 1.1 tip height setback. However,

as the setback multiplier increases further, the available area decreases enough that the number of turbines that can fit in the plant is much more limited. In these cases, the number of turbines is limited to not be able to reach the minimum COE value, represented for the conservative turbine in Fig. 9. For the conservative turbine, the optimal number of turbines can still be placed in the plant with a setback of 2, but the capacity is reduced by about 20% for the setback tip multiplier of 3. Because of the larger tip heights for the moderate and advanced turbines, the increasing setback multipliers decrease the available land for these turbines faster than for the conservative turbine. Also, the larger rotor diameters result in fewer suitable turbine locations that do not violate minimum spacing constraints. Thus, the optimal capacity for the larger turbines is more sensitive to the increasing setback multiplier. For the moderate turbine, a setback of 2 decreases the optimized capacity about 20% compared to the 0 setback case, and a setback of 3 decreases the optimal capacity more than 60%. For the advanced turbine, a setback of 2 decreases the optimized capacity about 50% compared to the 0 setback case, and a setback of 3 decreases the optimal capacity about 70%.

Next, for the objective of minimizing COE, we will explore the sensitivity of optimal COE to the setback constraint for the different turbines. As with the optimal capacities, there is very little difference between the optimal COE between the 0 setback and 1.1 setback constraint. The increase in COE at the larger setbacks is caused mostly by the decrease in capacity, which causes an increase in the unit costs. For the conservative innovation turbine, the very slight increase in COE from a setback of 1.1 to 2 is caused by increased wake interactions between turbines. In this case, the optimal number of turbines can still fit in the wind plant, but the

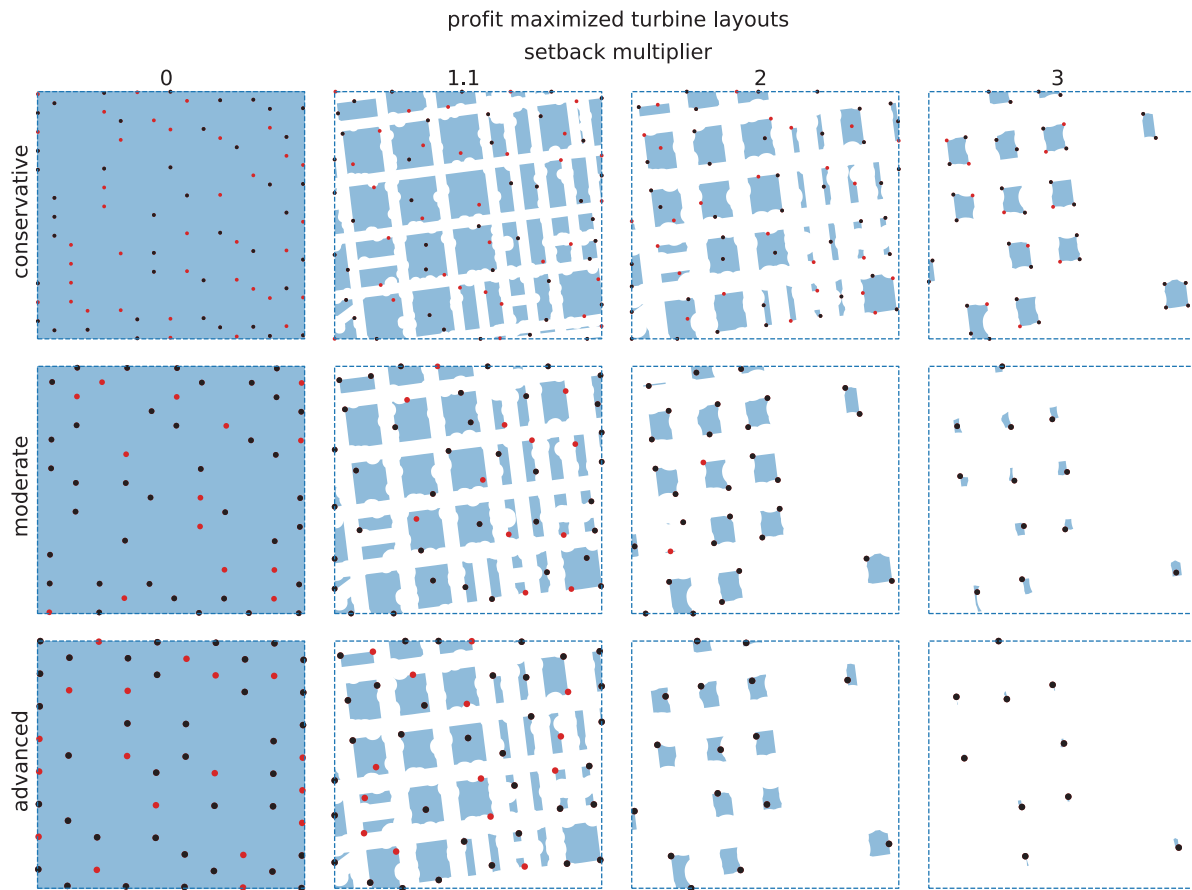


**Fig. 12.** The optimal wind plant layouts with the objective of maximizing profit. The black points show the optimal turbine locations for minimizing COE. These turbines also exist in the layout to maximize profit. The red points indicate the additional turbines in this layout compared to the minimum COE layout. The rows from top to bottom show the conservative, moderate, and advanced innovation turbines, where the size of each black dot is to scale representing the turbine rotor diameter. The columns from left to right show setback tip height multipliers of 0, 1.1, 2, and 3. We used PPA values of 51.22, 38.91, and 30.27 \$/MWh for the conservative, moderate, and advanced turbines, respectively.

more limited area means that the turbines are closer together, and thus have higher wake losses.

Finally, we will discuss the relationship of optimal wake loss in the wind plant as a function of the setback tip height multiplier, for each turbine. As with the capacity and COE, the wake losses between a setback multiplier of 0 and 1.1 are very similar. For the conservative innovation turbine, the wake losses slightly increase from the setback multipliers of 1.1 to 3. For these setbacks, the number of turbines is the same or almost the same as the 1.1 setback case, except the land area is more limited. This drives the turbines closer together and increases wake losses. This same reasoning causes the wake losses to increase for the moderate innovation turbine at a setback of 2. For the moderate innovation turbine at a setback of 3, and the advanced innovation turbine at setbacks of 2 and 3, the wake losses drop dramatically compared to the 0 setback case. For these optimized wind plants, the land area is so limited that there are very few turbines placed in the plant as evidenced by the extreme drop in capacity. In these cases, the wake losses decrease because of the small number of turbines and their large separation.

In general, increasing turbine tip height results in larger relative changes in capacity, COE, and wake losses for this example site and site-specific siting constraints. If turbine cost per unit capacity decreases with turbine rating (assuming a constant specific power), lower absolute COE values may result, depending on siting constraints. It is important to note that we have assumed the NREL ATB turbines, which have decreasing costs as turbine size increases. Fig. 12 shows the absolute values for COE and other

variables for a COE objective for the three turbines. The turbine cost decreases on a per capacity basis from the conservative to moderate and advanced cases. Therefore, the turbine resulting in the lowest COE or highest profit may vary in size and rating depending on the relationship of turbine cost as a function of rating in this simplified example. Considerations of site suitability for resource, turbulence, hub height, turbine market pricing and availability, turbine component transportation, constructability, and ownership model will influence the turbine characteristics selected for a specific site.

While Figs. 13 and 14 show the full and relative results for the wind plants optimized for minimum COE, Figs. 15 and 16 similarly show metrics from the wind plants optimized for maximum profit. As with the optimal COE figures, the optimal profit figures show results for each turbine and setback multiplier. Before examining some of the most important trends that we have identified, it is important that we point out one important observation about these results. For the advanced innovation turbine at a setback tip height multiplier of 3, the optimized profit is negative. With the extremely limiting setback constraints, there is not enough available land to build enough turbines to gain significant advantages from the economies of scale. Clearly, we can see that this is suboptimal, for it would be better to build zero turbines rather than lose money. The optimizer found the negative solution because it is a local maximum of profit. Subtracting a single turbine would result in even greater losses because of the sharp increase in plant costs per capacity that occurs at low wind plant capacities. The negative profit optimization is indicated by

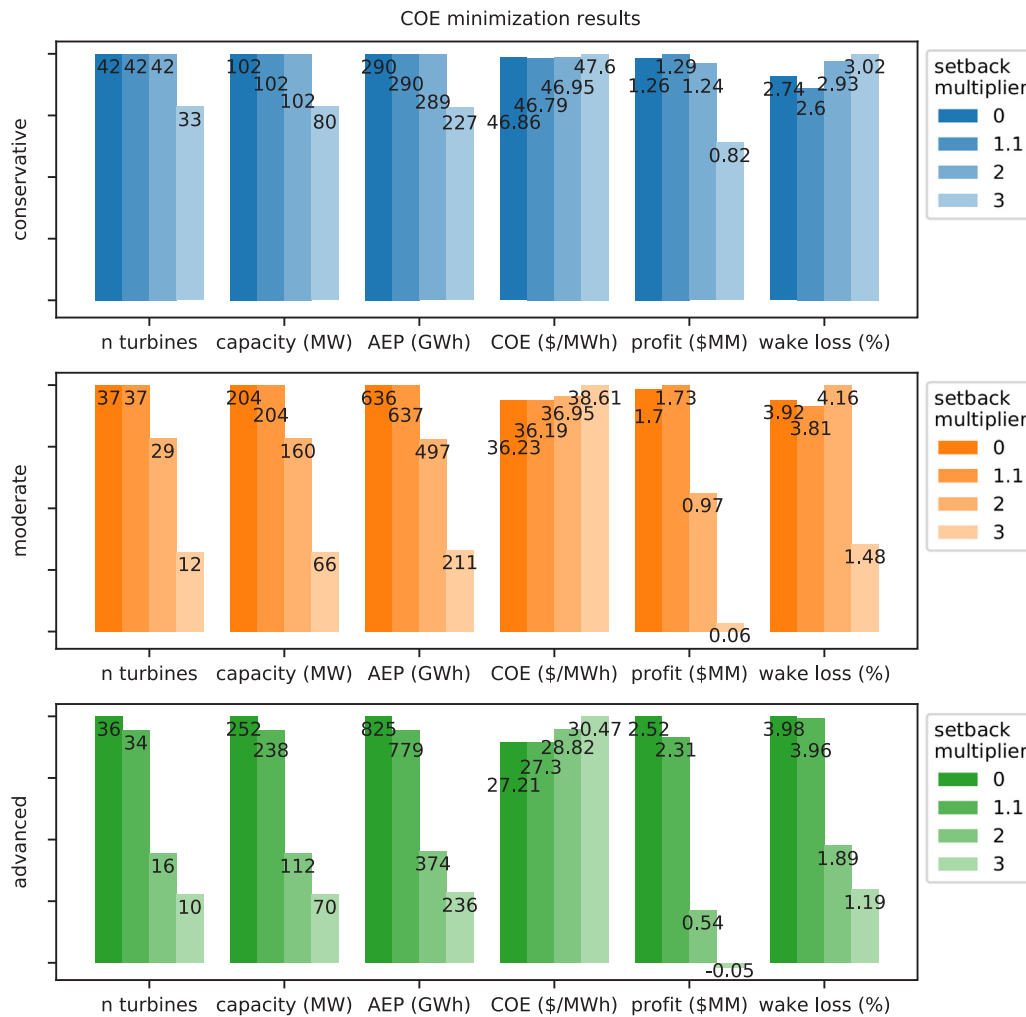


**Fig. 13.** Various metrics of the optimized wind plant for the objective of minimizing COE. From left to right, the metrics shown are optimal number of turbines (n turbines), capacity, AEP, COE, annual profit, and wake loss. From top to bottom, each subplot shows the results for the conservative, moderate, and advanced innovation turbines. The different shades of colors show optimal results for different setback tip height multipliers, indicated in the legends. (For interpretation of the references to color in this figure legend, the reader is referred to the web version of this article.)

the gray stripes through affected results in Fig. 15, and the black circles around the affected results in Fig. 16.

The trends seen in Fig. 16 have a lot in common with those in Fig. 14. First, when looking at the optimal plant capacities for the profit maximized plants, the capacity decreases for every turbine each time the setback constraint is increased. Although the increasing setbacks results in greater capacity decreases for the larger turbines, solutions for each turbine result in decreasing capacity. This indicates that even after applying the smallest setback constraint of 1.1 times the tip height, the land area is sufficiently limited that the optimal number of turbines to maximize profit can no longer fit in the plant. The relationship of COE as a function of the setback multiplier is very similar in Fig. 16 to Fig. 14. The COE increases as setback multiplier increases are mostly caused by the decrease in capacity due to less available land area. One interesting observation in Fig. 15 is that the COE for a setback of 1.1 is actually slightly lower than for the 0 setback. As we see in the optimal COE results, the slightly reduced capacity from the 1.1 setback is actually more optimal from a minimum COE perspective. However, when maximizing the profit, the slight decrease in COE does not make up for the loss of production.

Finally, we will discuss the trends of optimal profit as a function of setback multiplier in these wind plants. Like with capacity, even the smallest setback multiplier causes a decrease in profit

for each of the wind turbines. Also similar to the capacity results, for this wind plant and set of models, the profit for larger turbines is more sensitive to increasing setbacks—this is because the more land area is affected by increasing setbacks for the larger turbines, and the available land is more restricted by the minimum spacing constraints. The larger turbines produce larger changes in capacity and unit costs even with the larger associated reductions in wake losses.

### 5. Implications for capacity density

Determining the installed capacity density potential of wind is an important part of technical potential assessments as well as capacity expansion models and represent a significant driver in determining the contribution of wind energy in the future. Appropriately defining and estimating capacity density is important to encourage investments into wind technologies and to provide realistic expectations of regional deployment. Technical potential represents the achievable capacity and generation potential of a geographic region that takes into account system performance, land-use and environmental constraints, and resource availability. Technical potential is used by a variety of stakeholders, including researchers, wind energy developers, state and federal land managers, as well as state and federal policymakers

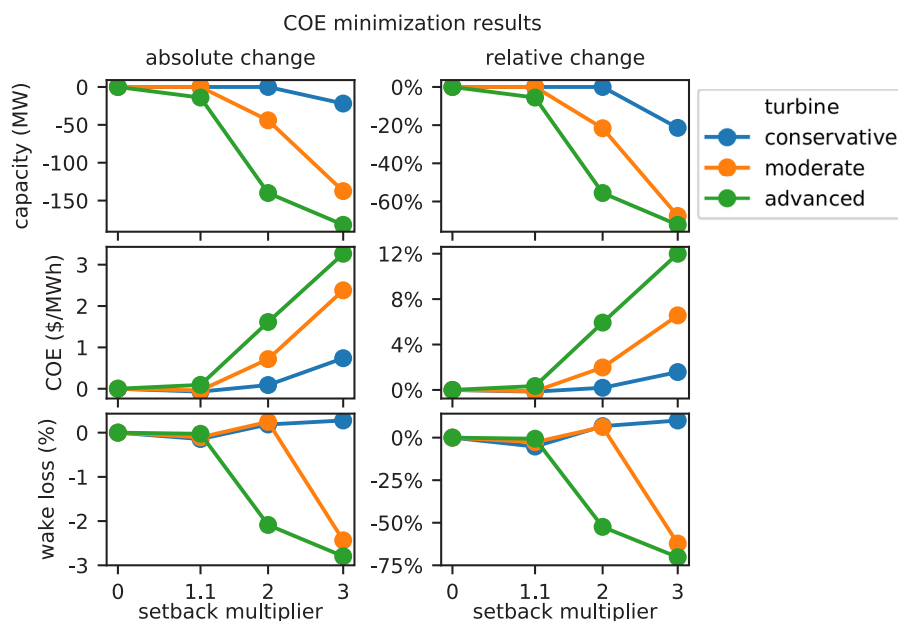


**Fig. 14.** The absolute and relative change for the metrics of capacity, COE, and wake loss for the wind plants optimized for minimum COE. Each color line shows results for each of the different turbines, given in the legend. Both the absolute and relative changes are given with respect to the metric value with zero setback constraints for the associated turbine. (For interpretation of the references to color in this figure legend, the reader is referred to the web version of this article.)

for setting renewable targets. It also underpins energy system models that explore pathways for wind energy integration. A key driver of technical potential is the assumed conversion of available land to capacity potential through use of a capacity density assumption.

Capacity density is defined as the installed capacity of a wind plant per unit area, which we will express with units of MW/km<sup>2</sup>. The installed capacity is easily understood as the sum of the rated capacities of the turbines within the wind plant. However, the area that should be used to represent wind plant capacity density is not as easily defined, and differing definitions have been used by past researchers (Denholm et al., 2009; Miller and Keith, 2018; Diffendorfer et al., 2019; Enevoldsen and Jacobson, 2021).

The confusion arises in whether the area occupied by the wind turbines should be the entire footprint of the wind plant (total area within the wind plant boundary), or whether the areas that are required for installation and operation of each wind turbine (direct area) should be used to determine capacity density. Direct area impacts to land use include turbine foundation area, crane pads, roads, substations, rotor width, operation and maintenance buildings, and electrical interconnection lines. The total and direct area impacted for wind plants varies by turbine rating, number of turbines, and turbine spacing. Denholm et al. (2009), Diffendorfer et al. (2019). Capacity density is a critical metric for broadly understanding social and environmental land-use impacts associated with existing wind energy development. Our work is focused on informing future wind energy potential through use in technical potential and capacity expansion models that aim to estimate local, regional, and national deployment potential of wind energy. For these models, accounting for the area available and estimated capacity for a wind plant is critical to estimating the potential deployment of wind energy at the plant to national scale.

Although the majority of a wind plant is not occupied by a wind turbine, the space between turbines is important for optimal wind plant design. Additional turbines in a fixed area increase wake losses, reducing the energy capture per turbine, and adding turbines to a fixed area can decrease plant cost on a per unit capacity basis. Thus, wind plant developers will design their wind plant layout around siting constraints while

maximizing profit by optimizing around turbine type, number of turbines, construction costs, and wake losses. For these reasons, we conclude that using direct area to estimate capacity density for wind technical potential assessments is not appropriate—as seen in Enevoldsen and Jacobson (2021). In this paper, we focus on two different, and more appropriate, measures of wind plant capacity density that capture both the dynamics of wind plant operation and siting criteria. The first is by using the total area defined by the wind plant boundary (boundary area). The second is by using just the areas that are not restricted by the spatial constraints (available area). Both boundary area and available area are important measures for technical potential and capacity expansion models when studying wind deployment potential.

Figs. 17 and 18 show the optimal capacity densities for objectives of minimum COE and maximum profit for each turbine and for each setback constraint. In each of these figures, the top left subfigure shows the optimal wind plant capacities, and the top right subfigure shows the available area to place wind turbines after removing the area excluded due to setback constraints. The bottom left subfigure shows the wind plant capacity densities by using the total wind plant boundary area, and the bottom right subfigure shows the optimal capacity densities using the available wind plant area after removing the setback constraints.

Let us now discuss the similarities in Figs. 17 and 18. For both objectives, from a setback of 0 to 1.1 there is either no change in plant capacity or a very small decrease for the advanced turbine. As the setbacks increase further, there is a larger decrease in plant capacity. The large decreases in capacity occur when the setbacks become large enough to completely remove some of the discrete parcels from the available land. As the setback multiplier increases the total capacity for minimum COE and target profit become similar because of the physical limitations on where turbines can be located. These results show that as siting constraints increase or as setback multiplier increases, the total capacity of the plant generally decreases. As wind deployment increases in the United States, wind plants may be sited in areas with higher setback constraints due to limited transmission capacity. These results suggest that future wind plants may have lower capacities and capacity densities, and taller turbines may see a larger impact due to siting constraints.

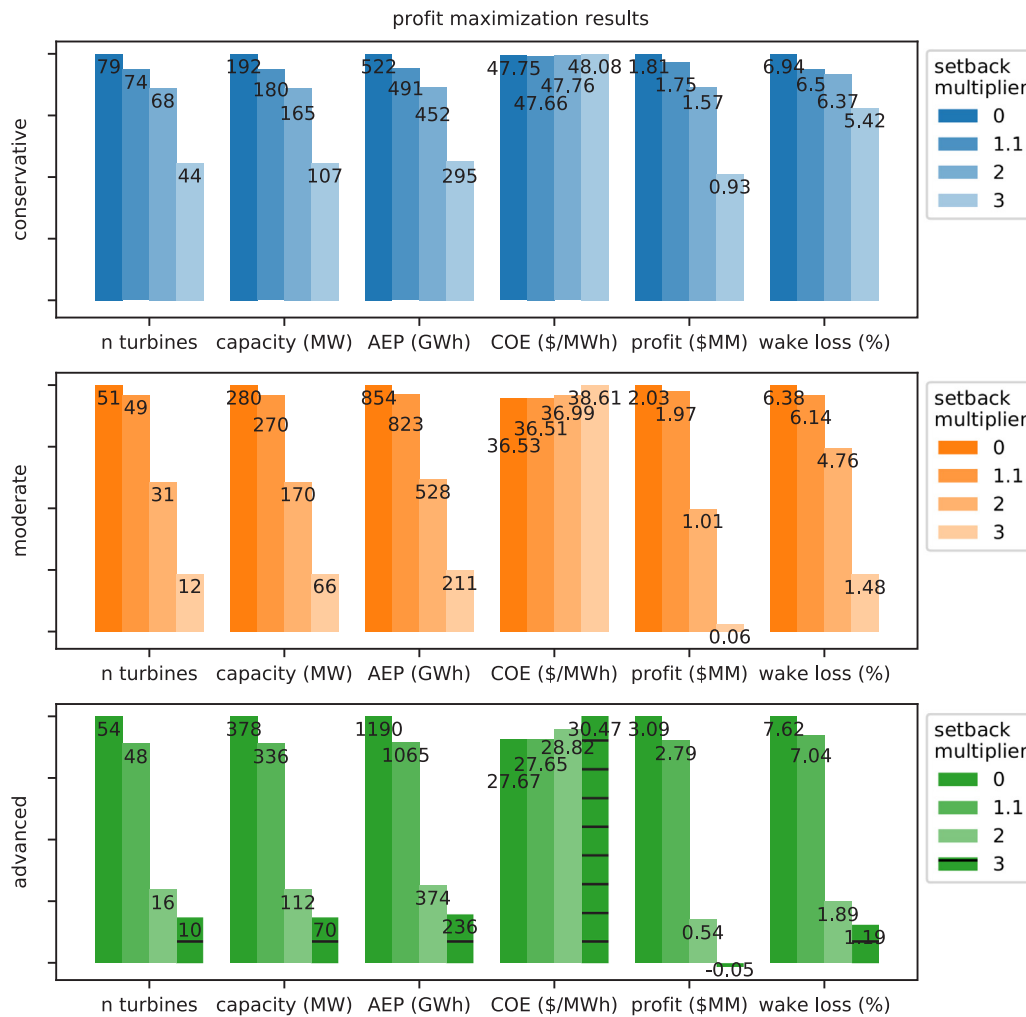


**Fig. 15.** Various metrics of the optimized wind plant for the objective of maximizing profit. From left to right, the metrics shown are optimal number of turbines (n turbines), capacity, AEP, COE, annual profit, and wake loss. From top to bottom, each subplot shows the results for the conservative, moderate, and advanced innovation turbines. The different shades of colors show optimal results for different setback tip height multipliers, indicated in the legends. The gray stripes represent an optimized wind plant where the profit is negative. (For interpretation of the references to color in this figure legend, the reader is referred to the web version of this article.)

Depending on the profit margin of the project, capacity density will vary with higher profit margins producing higher capacity densities but higher COE values. Empirically this is relevant as existing wind plants vary in capacity density due to many factors, with one being variations in profit margins. As profit margins, policy, incentives, etc., vary in the future, capacity densities resulting from specific target profit margins will vary. Fig. 19 shows the ratio of plant capacities for the profit and COE cases for each turbine by setback multiplier. With zero setbacks, the capacities for profit are between 1.3 and 1.9 larger than the capacities for the minimum COE case, which illustrates that when assuming a 10% profit for a wind plant the resulting capacity densities will be higher than for plants optimized for minimum COE. This is a critical point because minimum COE is typically used in wind energy research and analysis. These results also show this ratio decreases as setback multiplier increases causing the number of locations or parcels suitable for turbines to decrease.

### 6. Conclusions

In this paper, we developed a new modeling methodology that captures the interaction between critical variables of wind plant design, including wind turbine characteristics, costs, and varying

degrees of siting restrictiveness. We demonstrated the sensitivity of projected wind plant capacity, capacity density, and AEP to these critical variables. We showed that boundary and available area capacity densities are driven by either the balance of wake losses, plant cost and scaling relationships for sites with few siting constraints, or by the combination of wake losses and plant cost combined with turbine size and siting setbacks. Increasing turbine tip height results in higher sensitivities to capacity and COE. Relative to the 0 setback case, the advanced turbine capacity decreased by 70%, whereas the conservative turbine capacity decreased by 20%. Similarly, the change in COE is roughly 5 times greater for the advanced turbine relative to the conservative turbine as setback multiplier varies from 0 to 3.

Boundary area capacity densities are nearly constant for all turbines from 0 to 1.1 setback multipliers, but decrease as setback multiplier increases beyond 1.1. This trend illustrates the impact of increasing setback constraints. Available area capacity densities are highly sensitive to turbine tip height and setback multiplier, as well as the way the available area is distributed. Modeling available area and boundary area capacity densities represents a large challenge for technical potential and capacity expansion modeling efforts. The profit objective results in higher capacity densities than the COE objective by a factor between 1.3 and

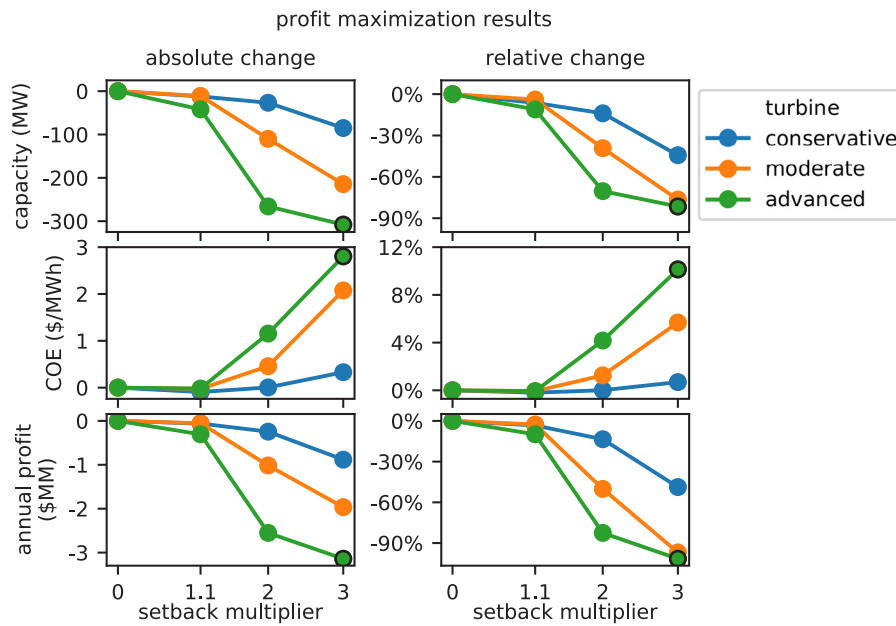


**Fig. 16.** The absolute and relative change for the metrics of capacity, COE, and annual profit for the wind plants optimized for maximum profit. Each color line shows results for each of the different turbines, given in the legend. Both the absolute and relative changes are given with respect to the metric value with zero setback constraints for the associated turbine. The green dots with the black outline represent an optimized wind plant where the profit is negative. (For interpretation of the references to color in this figure legend, the reader is referred to the web version of this article.)

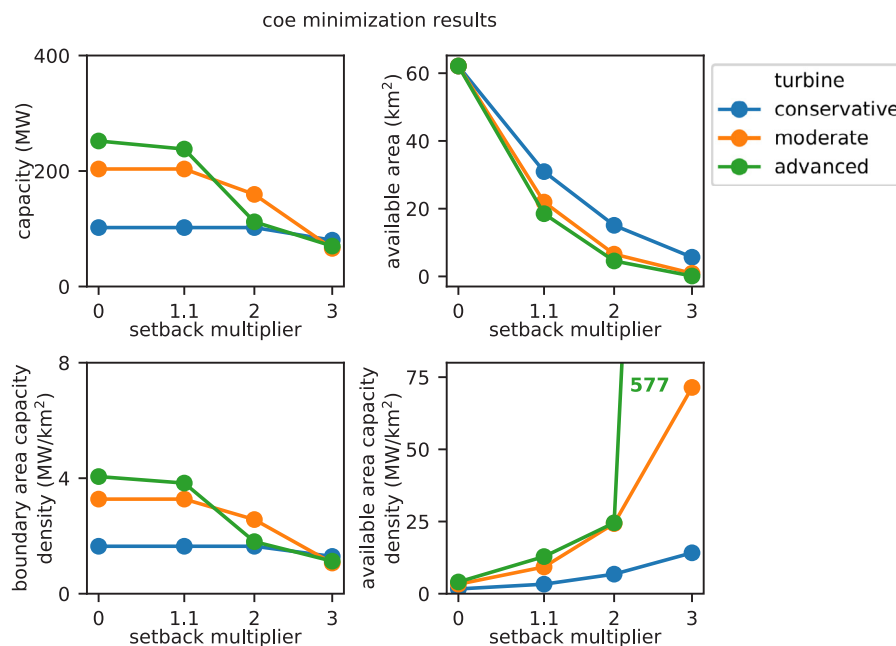


**Fig. 17.** Metrics related to the wind plant capacity density versus the setback tip height multiplier for plants optimized for minimum COE. The top left subplot shows optimized capacity, the top right shows the available area the place wind turbines after removing the setbacks, the bottom left shows the wind plant capacity density by using the wind plant boundary as the area, and the bottom right shows the wind plant capacity density by using the available area after setbacks (shown in the top right subplot) as the area. Each line color represents a different turbine indicated in the figure legend. (For interpretation of the references to color in this figure legend, the reader is referred to the web version of this article.)

1.9 for a 1.1 profit scenario relative to a minimum COE scenario. COE is a common objective for wind plant optimization; however, these results suggest that current capacity density assumptions underpredict boundary area capacity.

Another unique takeaway from this paper is our presented methodology for optimizing the number of turbines and their layout for different objectives in a boundary divided into discrete sections. We found that as siting constraints increase, the total

capacity of the plant generally decreases while COE increases. We show that larger and taller turbines produce higher sensitivities to plant capacity as turbine tip height setbacks increase. As wind deployment increases in the United States, wind plants may be sited in areas with higher setback constraints due to limited transmission capacity. These results suggest that future wind plants employing larger and taller turbines may have lower



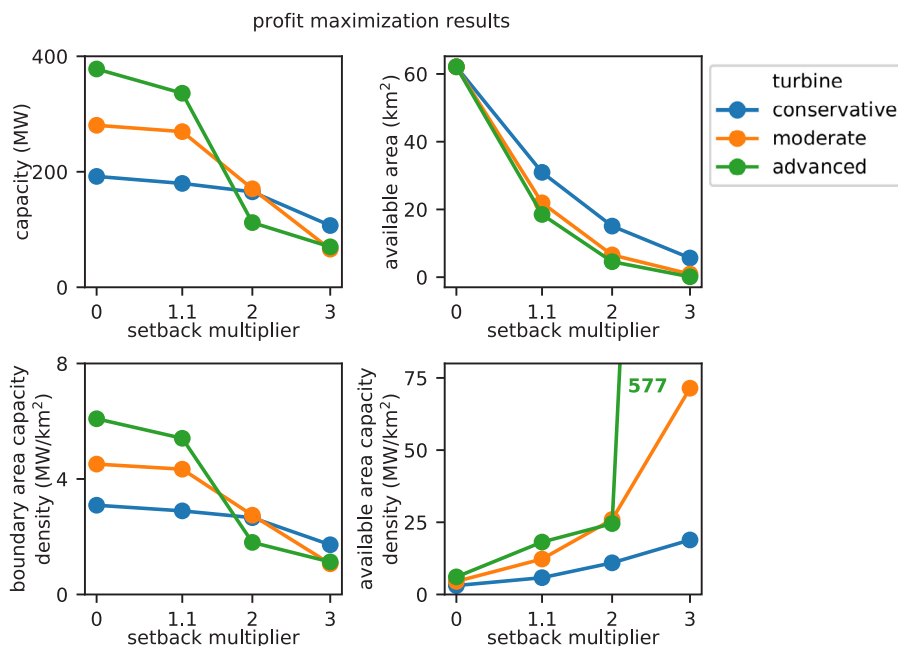


**Fig. 18.** Metrics related to the wind plant capacity density versus the setback tip height multiplier for plants optimized for maximum profit. The top left subplot shows optimized capacity, the top right shows the available area the place wind turbines after removing the setbacks, the bottom left shows the wind plant capacity density by using the wind plant boundary as the area, and the bottom right shows the wind plant capacity density by using the available area after setbacks (shown in the top right subplot) as the area. Each line color represents a different turbine indicated in the figure legend. (For interpretation of the references to color in this figure legend, the reader is referred to the web version of this article.)

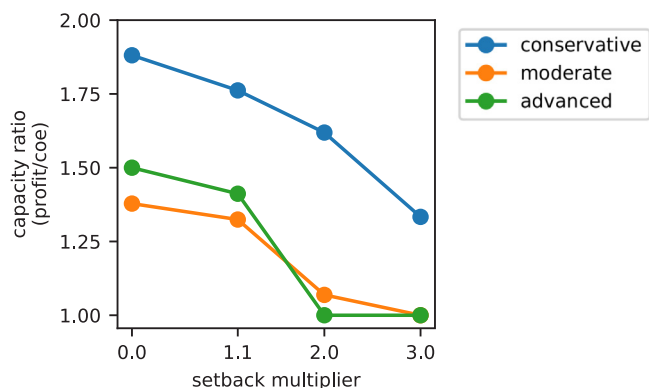


**Fig. 19.** The ratio of wind plant capacities for the plants optimized for maximum profit divided by the plants optimized for minimum COE. This figure indicates that a profit objective results in higher capacities than a COE objective. Each line color represents a different turbine indicated in the figure legend. (For interpretation of the references to color in this figure legend, the reader is referred to the web version of this article.)

capacities, capacity densities, and higher COE values due to siting constraints. These relationships – combined with land-based wind turbine size and tip heights increasing – are critical to understand the influences of local turbine setback legislation and as turbine scale changes. Meeting aggressive decarbonization goals with large deployments of land-based wind requires additional research to understand and inform stakeholders and policymakers. These results show large sensitivities of capacity, capacity densities, profit, and COE to turbine size, setback multiplier, and existing structures. Continued research through technical potential and capacity expansion modeling incorporating these methods and results is critical to fully understand future wind deployment scenarios.

### 7. Future work

This area of study is increasing in relevance as turbine scales increase, turbine costs decrease, wind COE falls, and decreases in transmission availability force projects into more populated or ecologically sensitive areas. This body of work and potential future work can also be valuable to develop turbine and plant characteristic assumptions for forward looking models, including NREL’s ATB. Of the many directions that could be considered for continuation of this work, in this section we present four specific areas of study that we believe are most relevant and impactful.

First is the development of a reduced order model for predicting variations in capacity density of wind plants from changes in turbine cost and scale, profit, wind resource, specific power, and innovations such as wake steering. The method of optimization presented in this paper is effective and computationally efficient when considering the optimization of a single site. However, it is infeasible to apply this same method to study wind capacity density for thousands of sites nationwide or even worldwide. This reduced order model would be used in national assessments of wind technical potential and capacity expansion models to more accurately predict future wind deployment pathways under deep decarbonization scenarios.

Second is to further refine the optimization methods for environmental impact constraints or objectives. As the deployment of wind rises dramatically, it will become increasingly important to develop metrics and methods to optimize wind farm layouts for high performance with minimal environmental impact. A potential formulation of this problem could be one where the siting limitations are not fixed, but there is a requirement that a certain portion of the wind farm area remain undeveloped.

Third is to couple turbine design variables within the wind farm layout optimization problem. Our past studies have demonstrated that when the number of turbines is fixed, coupled turbine design and layout optimization performs better than optimizing these sequentially. Further benefits can be gained if turbines are

optimized individually, allowing multiple turbine designs within the wind farm (Stanley and Ning, 2019a). Coupled turbine design and layout optimization while exploring the optimal number of turbines, setback constraints, and different objectives could be an interesting and important area to research.

Fourth is to consider further innovations that can effect wind deployment. Two specific innovations that we think are important to mention are wake steering through yaw misalignment, and advanced plant controls to mitigate the impacts of flicker and noise. Wake steering can be used to either increase production in existing farms, or to build turbines closer together with lower wake losses and wake induced turbine loads. This could increase siting flexibility and capacity density, and affect the sensitivities that we explored for this paper. Advanced plant controls could be used to reduce the required setback requirements imposed on turbines. As shown in this paper, reducing setbacks could increase the potential of wind and greatly impact future deployment.

### Code availability

The code and optimized data for this specific paper can be found at:

<https://github.com/pjstanle/spatial-optimization>

This repository includes the optimal layouts, run scripts, and optimizer used for this research.

The open source simulation code HOPP can be found at:

<https://github.com/NREL/HOPP>

### CRedit authorship contribution statement

**Andrew P.J. Stanley:** Methodology, Software, Investigation, Writing – original draft, Visualization. **Owen Roberts:** Conceptualization, Methodology, Writing – original draft. **Anthony Lopez:** Conceptualization, Writing – original draft, Supervision, Project administration, Funding acquisition. **Travis Williams:** Data curation, Writing – review & editing, Visualization. **Aaron Barker:** Methodology, Software, Writing – review & editing.

### Declaration of competing interest

The authors declare that they have no known competing financial interests or personal relationships that could have appeared to influence the work reported in this paper.

### Acknowledgments

We thank John Jasa, Trieu Mai, Eric Lantz, Christopher Bay, Patrick Gilman, and Gage Reber for their thoughtful and constructive feedback throughout the development of this work, and in providing reviews for earlier drafts. This work was authored by researchers from the National Renewable Energy Laboratory, operated by Alliance for Sustainable Energy, LLC, for the U.S. Department of Energy (DOE) under Contract No. DE-AC36-08GO28308. Funding provided by U.S. DOE Office of Energy Efficiency and Renewable Energy Wind Energy Technologies Office. The views expressed in the article do not necessarily represent the views of the DOE or the U.S. Government. Any errors are the sole responsibility of the authors. The U.S. Government retains and the publisher, by accepting the article for publication, acknowledges that the U.S. Government retains a nonexclusive, paid-up, irrevocable, worldwide license to publish or reproduce the published form of this work, or allow others to do so, for U.S. Government purposes.

### References

- Baker, N., Ning, A., Thomas, J., Stanley, A.P.J., 2021. *iea37-wflo-casestudies*. <https://github.com/byuflowlab/iea37-wflo-casestudies/blob/master/cs3-4/iea37-cs3-announcement.pdf>.
- Baker, N.F., Stanley, A.P., Thomas, J.J., Ning, A., Dykes, K., 2019. Best practices for wake model and optimization algorithm selection in wind farm layout optimization. In: *AIAA Scitech 2019 Forum*. p. 0540.
- Center, B.P., 2020. *Annual Energy Outlook 2020*. Energy Information Administration, Washington, DC.
- Chen, L., MacDonald, E., 2011. A new model for wind farm layout optimization with landowner decisions. In: *International Design Engineering Technical Conferences and Computers and Information in Engineering Conference*, Vol. 54822. pp. 303–314.
- Chen, L., MacDonald, E., 2012. Considering landowner participation in wind farm layout optimization.
- Chen, L., MacDonald, E., 2013. Effects of uncertain land availability, wind shear, and cost on wind farm layout. In: *International Design Engineering Technical Conferences and Computers and Information in Engineering Conference*, Vol. 55881. American Society of Mechanical Engineers, V03AT03A025.
- Chen, L., MacDonald, E., 2014. A system-level cost-of-energy wind farm layout optimization with landowner modeling. *Energy Convers. Manage.* 77, 484–494.
- Cole, W.J., Gates, N., Mai, T.T., Greer, D., Das, P., 2020. 2019 Standard Scenarios Report: A US Electric Sector Outlook. Tech. Rep., National Renewable Energy Lab (NREL), Golden, CO (United States).
- Denholm, P., Hand, M., Jackson, M., Ong, S., 2009. Land-Use Requirements of Modern Wind Power Plants in the United States. Tech. Rep., National Renewable Energy Lab (NREL), Golden, CO (United States).
- Diffendorfer, J.E., Dorning, M.A., Keen, J.R., Kramer, L.A., Taylor, R.V., 2019. Geographic context affects the landscape change and fragmentation caused by wind energy facilities. *PeerJ* 7, e7129.
- Draxl, C., Clifton, A., Hodge, B.-M., McCaa, J., 2015. The wind integration national dataset (WIND) toolkit. *Appl. Energy* 151, 355–366.
- Eberle, A., Roberts, O., Key, A., Bhaskar, P., Dykes, K., 2019. NREL's Balance-of-System Cost Model for Land-Based Wind. Tech. Rep., National Renewable Energy Lab (NREL), Golden, CO (United States).
- Enevoldsen, P., Jacobson, M.Z., 2021. Data investigation of installed and output power densities of onshore and offshore wind turbines worldwide. *Energy Sustain. Dev.* 60, 40–51.
- Eurek, K., Sullivan, P., Gleason, M., Hettinger, D., Heimiller, D., Lopez, A., 2017. An improved global wind resource estimate for integrated assessment models. *Energy Econ.* 64, 552–567.
- Freeman, J.M., DiOrio, N.A., Blair, N.J., Neises, T.W., Wagner, M.J., Gilman, P., Janzou, S., 2018. System Advisor Model (SAM) General Description (version 2017.9.5). Tech. Rep., National Renewable Energy Lab (NREL), Golden, CO (United States).
- Gillies, S., et al., 2007. Shapely: Manipulation and analysis of geometric objects. URL <https://github.com/Toblerity/Shapely>.
- HIFLD Open Data, 2020. Homeland infrastructure foundation-level data (HIFLD). <https://hifld-geoplatform.opendata.arcgis.com>. (Accessed 12 October 2020).
- Hou, P., Zhu, J., Ma, K., Yang, G., Hu, W., Chen, Z., 2019. A review of offshore wind farm layout optimization and electrical system design methods. *J. Mod. Power Syst. Clean Energy* 7 (5), 975–986.
- Jensen, N.O., 1983. A Note on Wind Generator Interaction. Citeseer.
- Lopez, A., Mai, T., Lantz, E., Harrison-Atlas, D., Williams, T., MacLaurin, G., 2021. Land use and turbine technology influences on wind potential in the United States. *Energy* 223, 120044.
- Lopez, A., Roberts, B., Heimiller, D., Blair, N., Porro, G., 2012. US Renewable Energy Technical Potentials. A GIS-Based Analysis. Tech. Rep., National Renewable Energy Lab (NREL), Golden, CO (United States).
- Mai, T., Lopez, A., Mowers, M., Lantz, E., 2021. Interactions of wind energy project siting, wind resource potential, and the evolution of the US power system. *Energy* 223, 119998.
- Microsoft, 2020. US building footprints. <https://github.com/Microsoft/USBuildingFootprints>. (Accessed 28 May 2020).
- Miller, L.M., Keith, D.W., 2018. Observation-based solar and wind power capacity factors and power densities. *Environ. Res. Lett.* 13 (10), 104008.
- Mosetti, G., Poloni, C., Diviacco, B., 1994. Optimization of wind turbine positioning in large windfarms by means of a genetic algorithm. *J. Wind Eng. Ind. Aerodyn.* 51 (1), 105–116.
- Nitsch, F., Turkovska, O., Schmidt, J., 2019. Observation-based estimates of land availability for wind power: a case study for Czechia. *Energy Sustain. Soc.* 9 (1), 1–13.
- NREL, 2020. 2020 Annual Technology Baseline (ATB) Cost and Performance Data for Electricity Generation Technologies. Tech. Rep., National Renewable Energy Lab (NREL), Golden, CO (United States), <https://data.nrel.gov/submissions/145>.
- Rinne, E., Holttinen, H., Kiviluoma, J., Rissanen, S., 2018. Effects of turbine technology and land use on wind power resource potential. *Nat. Energy* 3 (6), 494–500.

- Stanley, A.P., Ning, A., 2019a. Coupled wind turbine design and layout optimization with non-homogeneous wind turbines. *Wind Energy Sci.* 4 (1), 99–114. <http://dx.doi.org/10.5194/wes-4-99-2019>.
- Stanley, A.P., Ning, A., 2019b. Massive simplification of the wind farm layout optimization problem. *Wind Energy Sci.* 4 (4), 663–676.
- Stanley, A.P., Roberts, O., King, J., Bay, C.J., 2021. Objective and algorithm considerations when optimizing the number and placement of turbines in a wind power plant. *Wind Energy Sci. Discuss.* 1–38.
- Stehly, T.J., Beiter, P.C., 2020. 2018 Cost of Wind Energy Review. Tech. Rep., National Renewable Energy Lab (NREL), Golden, CO (United States).
- Thomas, J.J., Ning, A., 2018. A Method for Reducing Multi-Modality in the Wind Farm Layout Optimization Problem, Vol. 1037, No. 4. IOP Publishing, 042012.
- Tripp, C., Guittet, D., King, J., Barker, A., Hamilton, B., 2020. Hybrid optimization and performance platform (HOPP). <http://dx.doi.org/10.11578/dc.20210326.1>, <https://github.com/NREL/HOPP>.
- Wang, L., Tan, A.C., Cholette, M.E., Gu, Y., 2017. Optimization of wind farm layout with complex land divisions. *Renew. Energy* 105, 30–40.
- Williams, J.H., Jones, R.A., Haley, B., Kwok, G., Hargreaves, J., Farbes, J., Torn, M.S., 2021. Carbon-neutral pathways for the United States. *AGU Adv.* 2 (1), e2020AV000284.